DSCC2013-3984

ONLINE ADAPTIVE RESIDUAL MASS ESTIMATION
IN A MULTICYLINDER RECOMPRESSION HCCI ENGINE

Jacob Larimore,[*] **Shyam Jade, Erik Hellström,**
Anna G. Stefanopoulou
University of Michigan
Ann Arbor, Michigan 48109
{larimore, sjade, erikhe, annastef}@umich.edu

Julien Vanier, Li Jiang
Robert Bosch LLC
Farmington Hills, Michigan 48331
{julien.vanier, li.jiang}@us.bosch.com

ABSTRACT

This work presents two advances to the estimation of homogeneous charge compression ignition (HCCI) dynamics. Combustion phasing prediction in control-oriented models has been achieved by modeling the in-cylinder temperature and composition dynamics, which are dictated by the large mass of residuals trapped between cycles. As such, an accurate prediction of the residual gas fraction as a function of the variable valve timing is desired. Energy and mass conservation laws applied during the exhaust valve opening period are complemented with online in-cylinder pressure measurements to predict the trapped residual mass in real time. In addition, an adaptive parameter estimation scheme uses measured combustion phasing to adjust the residual mass prediction. Experimental results on a multicylinder gasoline HCCI engine demonstrate the closed loop residual estimation's ability to compensate for modeling errors, cylinder to cylinder variations, and engine wear. Additionally it is shown that using the adaptive parameter estimation reduces the model parameterization effort for a multicylinder engine.

INTRODUCTION

Recompression homogeneous charge compression ignition (HCCI) is a promising combustion strategy that can achieve high thermal efficiency with low engine-out emissions. It is characterized by compression-driven near simultaneous auto-ignition events at multiple sites throughout a homogeneous mixture. Auto-ignition timing control in HCCI combustion requires careful regulation of the temperature, pressure, and composition of the pre-combustion cylinder charge. This regulation of charge properties is carried out in recompression HCCI by retaining a large frac-

tion of the post-combustion residual gases before they can be exhausted [1,2].

Since neither the temperature nor the mass of the trapped residuals can be measured directly, model-based control of recompression HCCI requires the development of accurate control-oriented models that can be run in real-time on embedded control hardware. Examples of HCCI control-oriented models can be found in literature [3–9]. The combustion phasing prediction accuracy of these models is especially crucial when they are used in model-based predictive control strategies, for example [9–12]. This is because the phasing, or timing, of HCCI combustion must be maintained within a narrow acceptable range to satisfy stability and mechanical constraints. The models must be robust to engine aging, parameter drift and changes in environmental conditions.

The current work advances the state of art in two important ways. First, the authors propose a novel, physics-based method of calculating the residual gas mass in real-time. Second, an adaptive parameter estimation scheme is implemented in a previously developed HCCI model [8,9], and is shown in experiments to improve prediction performance and robustness.

Accurate modeling of the residual gas fraction is important for a control oriented model due to HCCI's high sensitivity to the thermal energy associated with the residual gases. If too much residual mass is trapped the combustion can occur very early causing potential engine damage and a loss in efficiency. If too little mass is trapped the combustion can become highly oscillatory [13, 14], and misfires may occur. While there have been methods described in literature for estimating the residual mass [15–18], none have presented an algorithm capable of online implementation without the use of a steady-state assumption. This work aims to provide a solution to this problem.

In addition, adaptive parameter estimation is used to increase

---

[*]Address all correspondence to this author.

the model fidelity in terms of its ability to reject disturbances and modeling error. The current HCCI model requires parameterization which is non-trivial and time intensive. As the model is propagated to multiple cylinders this task can become even more arduous. It will be shown through experiments that a parameterization for a single cylinder is sufficient when the adaptive parameter estimation is used and that the adaptation can reject actuator bias effectively. Other advantages of using adaptation include reducing sensitivity to engine aging, cylinder-to-cylinder variation and unmodeled dynamics.

The paper is organized as follows: First the model and an additional state are derived. The adaptive parameter estimation routine is then presented followed by experimental results and conclusions. Appendicies include nomenclature and a summary of the model equations.

MODEL DEVELOPMENT

The following sections present the two state control oriented model developed in [8,9] and the derivation of an additional state for residual mass estimation. A parametric model for adaptive parameter estimation is also introduced.

Two State Model

The model consists of two dynamic states used to capture cycle to cycle interactions which are:

1. T_{bd}: The temperature of the blowdown gases, which is used to represent the recycled thermal energy.
2. b_{bd}: The burned gas fraction of the blowdown process, which represents the composition dynamics.

The blowdown process is a rapid expansion of exhaust gases during the exhaust stroke where the pressures of the cylinder and exhaust system equalize quickly. The states are defined immediately after the blowdown process and are given by Eq. (1) and (2). A summary of the equations from [8,9] from which these states are derived can be found in the appendix.

$$T_{bd}(k+1) = T_{evo}(k)\left(\frac{p_{evo}}{p_{em}}\right)^{\frac{1-n}{n}}$$
$$= T_{ivc}(k)\left(\frac{p_{ivc}(k)}{p_{em}}\right)^{\frac{1-n}{n}}\left[1 + \frac{\eta_m q_{lhv} R V_{50}{}^{n-1}}{c_v p_{ivc} V_{ivc}{}^n} m_f(k)\right]^{\frac{1}{n}} \quad (1)$$

$$b_{bd}(k+1) = \frac{(AFR_s + 1)m_f(k)}{m_c(k)} + x_r(k)b_{bd}(k) \quad (2)$$

The model has three inputs: the mass of fuel injected (m_f), the injection timing (SOI), and the timing of the exhaust valve closing (EVC). The EVC timing controls the amount of NVO, the crank angle difference between EVC and intake valve opening (IVO), with which the engine operates. This has a direct impact on the charge composition and temperature. The model has two
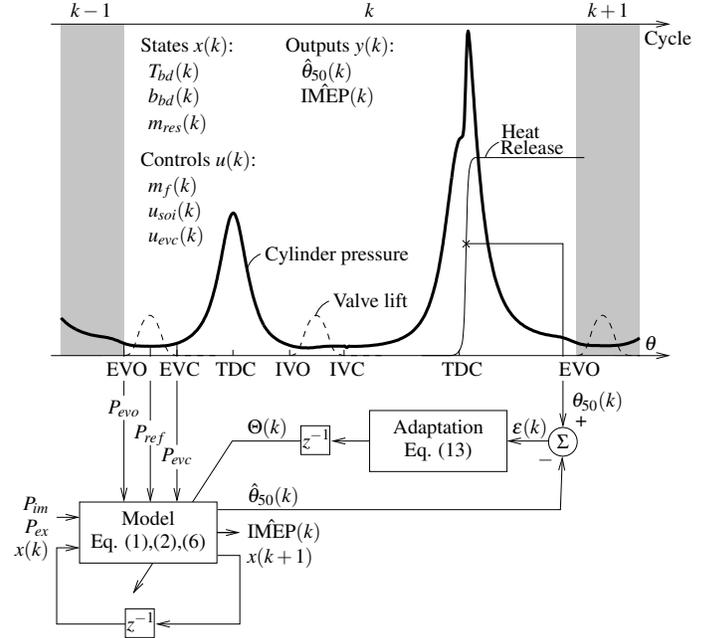

Figure 1. Graphical representation of model structure. The figure indicates when the time series data is broken into discrete elements, the model inputs and outputs as well as the states. Also shown is the basic block diagram of the model indicated what measurements are used.

outputs, the combustion phasing of 50% burn ($\hat{\theta}_{50}$) and the engine torque (IMEP). Therefore this is a three input two output system. A visual representation of the model is given in Fig. 1.

Residual Mass State

The hot residual mass trapped in recompression HCCI comprises a significant portion of the charge, and therefore thermal energy. Since the combustion depends on this thermal energy, accurate prediction of the residual mass is imperative. Previously, the model's formulation of residual mass was a static function of EVC, manifold pressures, engine speed and the state T_{bd} which was tuned using steady state data. The function can be found in Eq. (26) of the appendix. The regression can be complicated to parameterize and does not benefit from knowledge of in-cylinder pressure measurements which provide the most direct information available about the combustion process in real time. It is therefore desired to develop a state for the residual mass which can take advantage of these measurements to increase model fidelity.

The residual mass state is derived using the offline analysis techniques presented in [15, 19] as a basis. To summarize, an analysis of the heat loss per unit mass due to the exhaust is performed by splitting it into two segments of equal time. It is physically reasonable to assume that the heat (and therefore mass) losses in the first and second halves of the exhaust will be similar, i.e. $q(evo \to ref) = q(ref \to evc)$ where the value of ref is the halfway point of the exhaust process in the crank angle domain defined as: $\theta_{ref} = (\theta_{evo} + \theta_{evc})/2$. Specifically these heat losses,

2 Copyright © 2013 by ASME

q, can be expressed as:

$$\int_{T_{evo}}^{T_{ref}} c_p dT - R \int_{P_{evo}}^{P_{ref}} \frac{T}{P} dP = \int_{T_{ref}}^{T_{evc}} c_p dT - R \int_{P_{ref}}^{P_{evc}} \frac{T}{P} dP,$$

where the values of P_x and T_x refer to the pressure and temperature inside the cylinder at specific locations in the cycle, for example $P_{evo} = P_{cyl}(\theta_{evo})$. After approximation of the integrals we have:

$$c_p(T_{ref} - T_{evo}) - R \left(\frac{T_{ref} + T_{evo}}{2} \right) \ln \left(\frac{P_{ref}}{P_{evo}} \right) =$$
$$c_p(T_{evc} - T_{ref}) - R \left(\frac{T_{evc} + T_{ref}}{2} \right) \ln \left(\frac{P_{evc}}{P_{ref}} \right).$$

Further, algebraic simplification yields:

$$\gamma T_{evo} + \zeta T_{evc} = T_{ref} \left\{ -2c_p + \frac{R}{2} \ln \left(\frac{P_{ref}^2}{P_{evo} P_{evc}} \right) \right\} \quad (3)$$

where: $\gamma = -c_p - \frac{R}{2} \ln \left(\frac{P_{ref}}{P_{evo}} \right)$, $\zeta = -c_p + \frac{R}{2} \ln \left(\frac{P_{evc}}{P_{ref}} \right)$.

Equation (3) has two unknowns, T_{evo} & T_{evc}, and other variables which are either known or can be measured with the exception of T_{ref}. The value of T_{ref} cannot be measured however it is close to the value of the blowdown temperature which is a state of this model, Eq. (1), and will be used as such. It is recognized that there maybe be discrepancy between the T_{ref} and T_{bd} values which provides motivation for the introduction of an adaptive parameter to make corrections to the model when necessary.

From here we deviate from the derivation in [19] by defining the unknown temperatures with the ideal gas law:

$$T_{evo} = \frac{P_{evo} V_{evo}}{m_{evo} R}, \quad T_{evc} = \frac{P_{evc} V_{evc}}{m_{evc} R},$$

and define the masses as follows:

$$m_{evo}(k) = m_{in}(k) + m_{res}(k), \quad m_{evc}(k+1) = m_{res}(k+1). \quad (4)$$

The transient residual mass, Eq. (4), can then be substituted into Eq. (3) which allows the masses to evolve in time and change from cycle-to-cycle depending on the manifold dynamics and cylinder conditions. The result is one equation in terms of $m_{res}(k)$ and $m_{res}(k+1)$

$$\gamma \frac{P_{evo} V_{evo}}{(m_{in}(k) + m_{res}(k))R} + \zeta \frac{P_{evc} V_{evc}}{m_{res}(k+1)R}$$
$$= T_{bd}(k) \left\{ -2c_p + \frac{R}{2} \ln \left(\frac{P_{ref}^2}{P_{evo} P_{evc}} \right) \right\}. \quad (5)$$

This equation can be greatly simplified by grouping terms and lumping constant coefficients:

$$m_{res}(k+1) = \frac{\alpha(k) + \beta(k) m_{res}(k)}{A(k) + m_{res}(k)} \quad (6)$$

where $\alpha(k)$, $\beta(k)$ and $A(k)$ are functions of the constants R and c_p, known inputs, T_{bd}, and measured values; namely the in-cylinder pressure at specific locations (P_{evo}, P_{evc} and P_{ref}) and the mass of fresh air inducted into the cylinder. By defining the masses as in
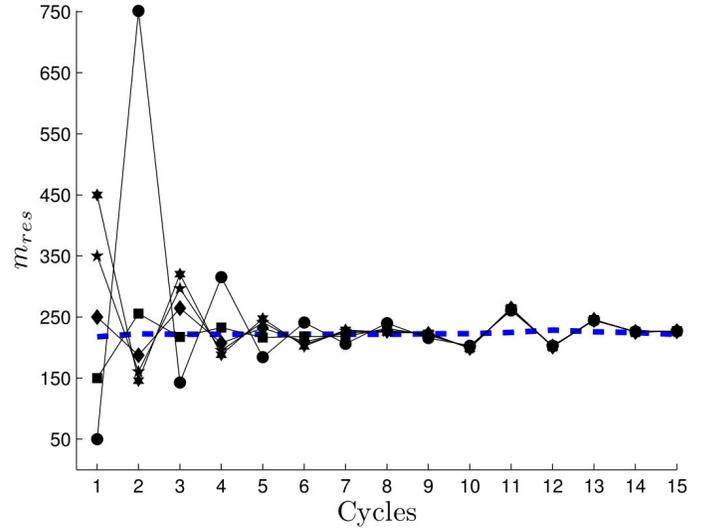

Figure 2. Convergence of the state m_{res}, in milligrams, from various initial guesses. Simulation was run at 1800 rpm and 3 bar IMEP.

(4) we accomplish three goals, first we no longer assume that the residual mass is in steady state, second, the equation depends on known, or measurable values. Finally, the equation is causal and sufficiently simple for online implementation.

The result found in Eq. (6) predicts the amount of residual mass in cycle $k+1$ based on measured data and the value of the residual mass in the previous cycle. Therefore, the only unknown is the initial guess of $m_{res}(0)$. A numerical example of the convergence from various initial guesses is given in Fig. 2. When the coefficients α, β and A are constant an equation of this form is referred to as the Riccati Difference equation [20]. For a given operating condition it is reasonable to assume that the coefficients will not change much from cycle to cycle and can be assumed constant. With this assumption it can be shown that for physically reasonable pressure data and a positive initial guess of residual mass, the state will converge to a stable, fixed–point equilibrium. The proof is omitted to conserve space, however a summary of this proof can be found in [20–22].

In summary, the model, augmented with the third state, in its functional form is given by:

$$T_{bd}(k+1) = f_1(T_{bd}(k), x_r(k), m_f(k), T_{im}, P_{int,exh} V, c_v) \quad (7a)$$
$$b_{bd}(k+1) = f_2(T_{bd}(k), x_r(k), m_f(k), b_{bd}(k)) \quad (7b)$$
$$m_{res}(k+1) = f_3(T_{bd}(k), m_{res}(k), P_{cyl}, V) \quad (7c)$$

where $x_r(k) = \frac{m_{res}(k)}{m_c(k)} = \frac{m_{res}(k)}{m_{res}(k) + m_{air}(k) + m_f(k)}$. \quad (8)

The values for T_{im}, P_{int}, T_{ex}, P_{exh} are the measured intake and exhaust temperatures and pressures respectively.

Parametric Model

The HCCI combustion model is not well suited for use with adaptive parameter estimation due to its highly non-linear re-

3

Copyright © 2013 by ASME

lationships and state couplings. As such, the placement of an adaptive parameter or parameters is challenging. In this section we develop a parametric model to adapt our prediction of x_r in Eq. (8) as defined by:

$$\hat{x}_r(k) = \Theta(k)x_r(k), \tag{9}$$

where $\Theta(k)$ is the adaptive parameter and $\hat{x}_r(k)$ is the new residual gas fraction to be used in the model. To determine the parameter $\Theta(k)$ we employ the influence that $\hat{x}_r$ has on T_{ivc} as shown in Eq. (10),

$$T_{ivc}(k+1) = \hat{x}_r(k)T_{res}(k) + (1-\hat{x}_r(k))T_{im}, \tag{10}$$

where T_{im} is a constant and T_{res} is from the model as in Eq. (29). This adapted residual gas fraction is also substituted into Eqs. (7a,b). In HCCI, the combustion phasing is directly influenced by the temperature of the charge at IVC. As such it makes physical sense to place an adaptive parameter into this regression to have the most direct influence over the prediction of the combustion phasing.

Equation (10) yields a parametric model by distributing terms and manipulating the equation into the from $\mu = \Theta\varphi$ where:

$$\mu = \frac{T_{ivc} - T_{im}}{T_{res} - T_{im}} \quad and \quad \varphi = x_r.$$

The value of T_{ivc} at this point is unknown and to form the error term, $\varepsilon = \mu - \hat{\Theta}x_r$, we must calculate an estimate of $T_{ivc,e}$ from measurements. This is done by inverting the model for combustion phasing prediction given by Eq. (17) using the calculated combustion phasing, θ_{50}, from a net heat release analysis done by the engine control unit (ECU) online:

$$T_{ivc,e} = \frac{-\alpha_{\theta 2} - \sqrt{\alpha_{\theta 2}^2 - 4\alpha_{\theta 1}(\alpha_{\theta 3} - \theta_{50})}}{2\alpha_{\theta 1}}. \tag{11}$$

The value of μ is then simply:

$$\mu = \frac{T_{ivc,e} - T_{im}}{T_{res} - T_{im}}. \tag{12}$$

ADAPTIVE LAW

The least squares algorithm with a forgetting factor follows from the derivation in [23, 24] and is summarized here:

$$\Theta(k) = \left(\sum_{i=1}^{k}\varphi(i)\kappa^{(k-i)}\varphi(i)^T\right)^{-1}\left(\sum_{i=1}^{k}\varphi(i)\kappa^{(k-i)}\mu(i)\right) \tag{13}$$

When $\kappa = 1$, this is the pure least squares algorithm. As κ is decreased there is more discounting of previous values but an increase in sensitivity to noise. To allow the parameter to change with operating conditions it is necessary to have some forgetting ($\kappa < 1$). Simulations for this model have shown that a value of $\kappa = 0.95$ is a good balance for the trade off of adapting to transients and rejecting noise. Other adaptive laws were also tested in simulation, specifically a pure least squares algorithm, a

least squares with covariance resetting and a gradient algorithm. However, least squares with forgetting factors provided the best balance of accuracy and noise suppression while still maintaining an ability to be implemented in real time.

It can be seen from induction that the sum in the denominator of Eq. (13) can be written as $D(k) = \kappa D(k-1) + \varphi(k)\varphi(k)^T$ and the sum in the numerator can be written as $N(k) = \kappa N(k-1) + \varphi(k)\mu(k)$. Since everything is scalar, $\Theta(k) = \frac{N(k)}{D(k)}$. There are two conditions to avoid: $D(k) = 0$ and either $N(k), D(K) \to \infty$. Since $D(k)$ is driven by φ^2, it will stay positive, provided it starts positive. Further, since $\varphi \in [0,1]$, $T_{res} \gg T_{im}$, and $\kappa < 1$, neither $N(k)$ nor $D(k)$ can grow indefinitely given physically reasonable data. To avoid unphysical behavior however, the value of Θ is also restricted to be within $\Theta \in [0.75, 1.25]$.

EXPERIMENTAL RESULTS

A four cylinder 2.0 liter GM LNF Ecotec engine running on premium grade indolene was used as the baseline platform. Modifications to accommodate HCCI combustion include increasing the compression ratio to 11.25:1 and using camshafts with shorter duration and lower lift to allow for unthrottled operation. In addition to the stock turbo charger the engine was augmented with a small supercharger (Eaton M24) to provide boost. Results presented here were run at slightly boosted conditions, approximately 1.1 bar intake manifold pressure, $\lambda = 1.2$, an engine speed of 1800 RPM and a load of approximately 3 bar net IMEP. The spark was left on, but at a position of $40°$ after top dead center. Since the mixture is lean and highly diluted with residuals the spark will have little influence on the combustion. Having the spark on late only helps to prevent the spark plug from fouling. Cylinder pressures were sampled at a resolution of 0.1 cad.

The model presented in this paper was implemented using a combination of C and Matlab code, and was tested in real-time using an ETAS ES910 rapid prototyping module. The module uses an 800 MHz Freescale PowerQUICC™ III MPC8548 processor with double precision floating point arithmetic and 512 MB of RAM. All experiments were run in open loop. Steady state experimental data was used to parametrize the model. However, the model was only tuned based on data for cylinder 1. This parameterization was propagated to all four cylinders on the rapid prototyping hardware despite the fact that there is cylinder-to-cylinder variation warranting a parameterization for each cylinder individually.

Because HCCI combustion must operate in a narrow band of combustion phasing, it is crucial that the control oriented model makes accurate predictions of the engine's phasing despite deviations from a nominal operating point or drift in parameters. As stated previously, the purpose of the adaptive model is to allow these changes to be captured. The adaptive law is driven by error between the predicted and measured θ_{50} and as such it should correct for these various errors. This will be shown through experimental results.

Copyright © 2013 by ASME

Multicylinder Results

Tuning the model is a difficult and time consuming task, in addition, the engine's parameters can drift on a day-to-day basis, it is therefore desired to be able to minimize this task and allow for the model to make adaptations online.

To test the adaptive model's capability to correct for modeling and parameterization errors it was run in real time at steady state conditions with and without adaptation while the response in predicted combustion phasing was observed. The results can be found in Fig. 3. Despite the model being parameterized for cylinder 1, day-to-day drift and uncontrollable changes in environmental conditions caused there to be a difference in the predicted versus calculated values. Cylinder number 2 also had large errors while cylinders 3 and 4 appear to have an accurate parameterization. Regardless, when adaptation is turned on at approximately cycle 200, the adaptive parameter makes adjustments to the model and the prediction of combustion phasing becomes more accurate. As expected, the adaptive parameter deviats from unity further when the error is larger, as is the case for cylinders 1 and 2. The RMS error, averaged over all four cylinders, between the predicted and actual values of combustion phasing with no adaptation was 2.51 cad while the RMS error with adaptation was 1.73 cad. Similar reductions in error were observed on all experimental results presented, there were no observations of the adaptive routine increasing RMS error of the combustion phasing.

It should be noted that when the prediction of residual gas fraction, $\hat{x}_r$, causes the model to predict a combustion phasing that is earlier than that of the ECU, then $\Theta < 1$. For the results presented here, the value of Θ was always less than one. This is due to the model always predicting a combustion phasing which is earlier than that of the actual value, an over prediction of the residual gas fraction. For a different parameterization of the model the prediction could have been later than the actual phasing, this would cause the adaptive parameter to be greater than 1. This was explored in simulations but did not present itself in experiments.

Single Actuator Steps

To evaluate the effectiveness of the adaptive model and residual gas fraction estimation in transients, actuator steps of the model inputs were performed in open loop. Sensor measurements were obtained in real time from the engine's ECU and used by the model for real time prediction of θ_{50}. The actuator steps were repeated for both the adaptive and non–adaptive model.

A step in EVC is shown in Fig. 4 for cylinder 1. The step is from 256 to $253°aTDC$ (degrees after top dead center) and back again and causes the amount of NVO to increase as a result. Intuitively, the amount of residual mass trapped in the cylinder should also increase, this is reflected in the prediction of the residual gas fraction as shown in Fig. 4. Also shown is the result of an offline analysis of the residual gas fraction derived from an iterative method described in [15, 19]. While the absolute difference between the two results is slightly different, the magnitude and direction of the transient response is similar. As described
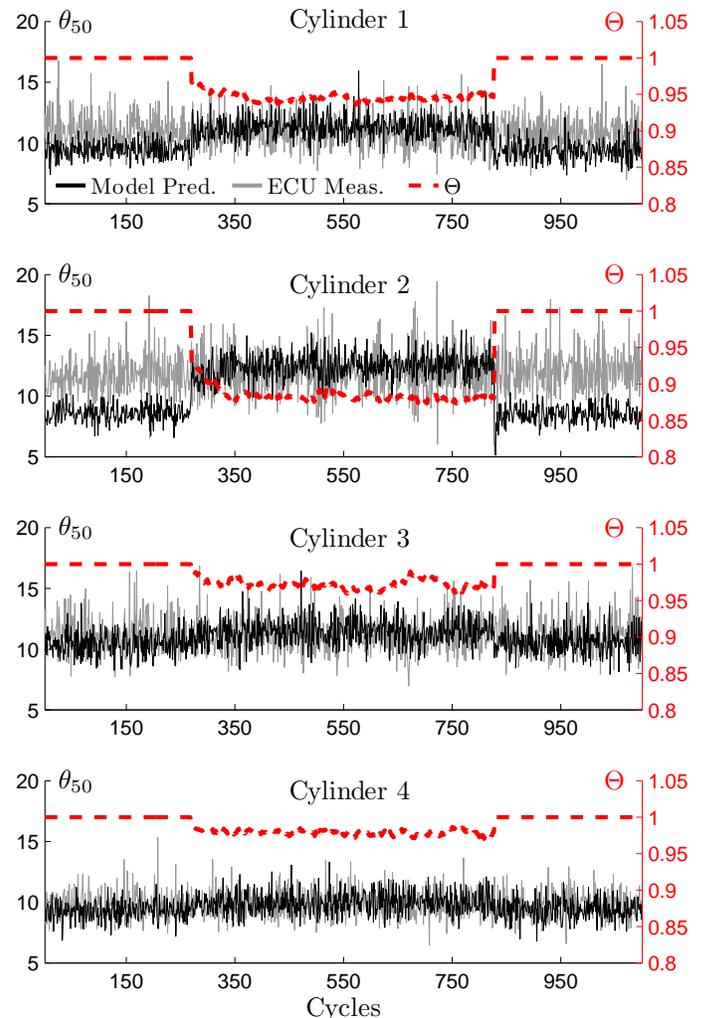

Figure 3. Combustion phasing prediction versus ECU calculation for the adaptive and non-adaptive versions of the model. It can be seen that with adaptation the error in combustion phasing is reduced.

in previous sections, it is expected that the absolute values may not be equal due to the difference in the value of the exhaust gas temperature and that of the state T_{bd}. As a consequence, the model prediction of θ_{50} differs from that of the ECU. However, when the adaptive parameter is introduced at approximately 1400 cycles, and the step is repeated, it is clear that the residual gas fraction drops to that of the offline analysis and the model prediction of θ_{50} becomes much more accurate on an absolute scale. It is not expected that the value of x_r always be equivalent to that of the offline processing except in the case of minimal modeling errors and environmental disturbances.

The model's response to steps in SOI and mass of fuel can be found in Figs. 5 and 6. The prediction of θ_{50} is improved in both responses. It should be noted that while the value of Θ stayed relatively constant during the EVC step, it has a visible response to the steps in SOI and fuel. This suggests that the
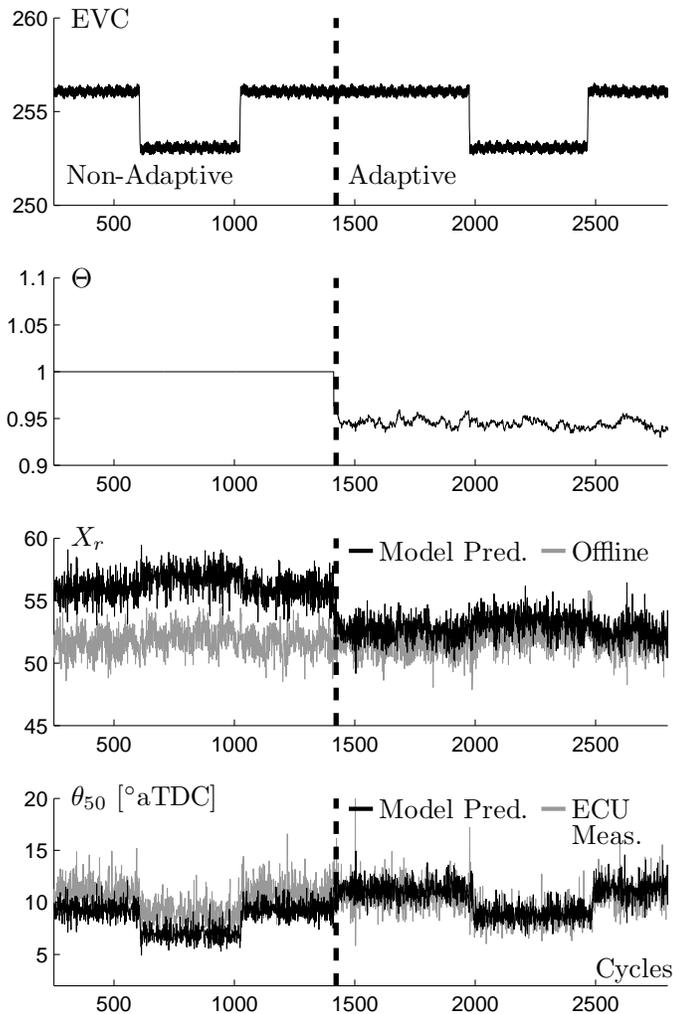
Figure 4. An EVC step for cylinder 1 with and without an adaptive model. It can be observed that the model prediction is more accurate when adaptation is applied.

model's parameterization may not fully capture the step response, however the adaptive parameter corrects for these errors.

Actuator Bias

It is common for engine components to wear and sensors to become more noisy with time, this can present a problem when running highly parameterized models online. It is therefore desired that the adaptive model be able to reject such disturbances. To test this the model was run online with the engine operating at steady state, all actuators fixed. The measurement of EVC used by the model was then replaced with one with a bias for a short period of time as seen in Fig. 7. This bias represents camshaft wear over time. One can see that when the bias is applied at 250 cycles that the combustion phasing prediction starts to deviate quickly from the calculated value. However, the adaptive parameter makes adjustments to the residual gas fraction in order to minimize the error. A similar response can be seen at 750 cycles when the bias
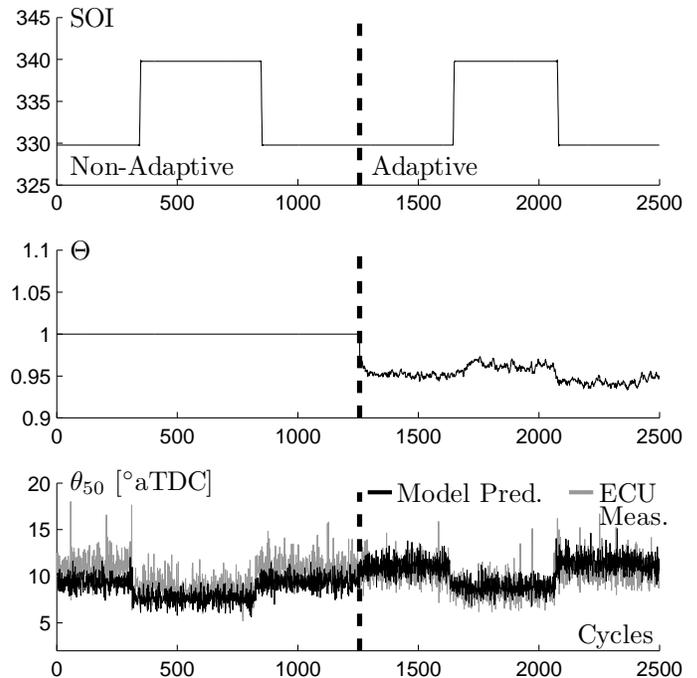

Figure 5. Model response to an SOI step with and without adaptation. When adaptation is applied the prediction of θ_{50} is more accurate.

is removed. In a more realistic scenario this bias will be slowly occurring over a long period of time as the cam is mechanically worn due to friction. Another example of this could be a parameter could drift over time, for instance engine temperature changing based on weather conditions. This experiment considers the worst case situation of the bias being applied instantaneously.

CONCLUSIONS

A physics-based method of computing the residual gas fraction of a recompression HCCI engine using cylinder pressure measurements in real time is presented along with an adaptive parameter estimation routine. It is important that the model predicts residual gas fraction trends accurately for control purposes. Experimental results show that the estimator of x_r captures expected trends well for single actuator steps and that with the adaptive algorithm, the absolute value of x_r is comparable to that of a higher fidelity, offline analysis.

In addition to correcting the residual gas fraction prediction to match offline analysis, the adaptive routine helps to mitigate errors in the prediction of combustion phasing in the presence of many sources of error by creating a nonlinear estimator of the model states. It has been shown that a single parameterization may be sufficient for a multicylinder engine using an adaptive parameter. Also, the algorithm can reject errors due to engine wear or parameter drift.
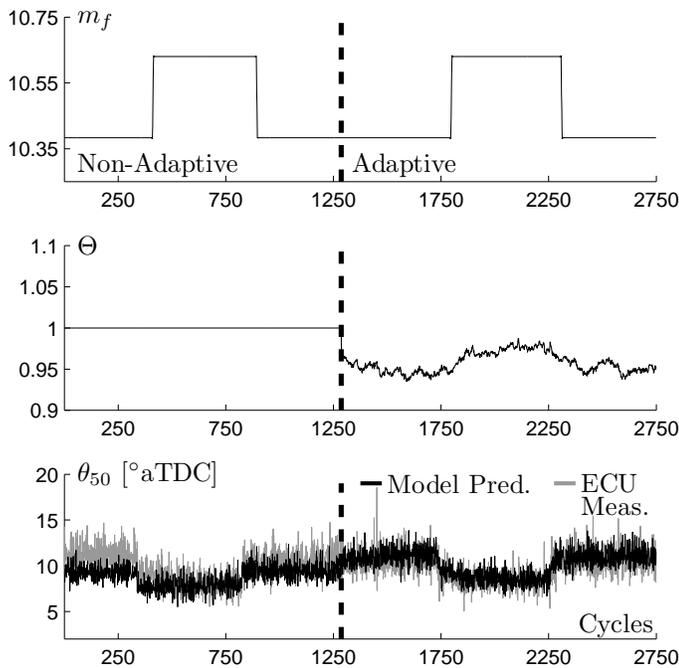
6   Copyright © 2013 by ASME

Figure 6. Model response to fuel mass step with and without adaptation.

ACKNOWLEDGMENT

References

[1] Yao, M., Zheng, Z., and Liu, H., 2009. "Progress and recent trends in HCCI engines". *Prog. in Ener. and Comb. Sci.,* **35**(5), Oct., pp. 398–437.

[2] Willand, J., Nieberding, R., Vent, G., and Enderle, C., 1998. "The knocking syndrom – its cure and its potential". *SAE Technical Papers,* **982483**.

[3] Shaver, G., and Gerdes, J., 2003. "Cycle-to-cycle control of HCCI engines". *ASME International Mechanical Engineering Congress and Exposition*(IMECE 2003-41966).

[4] Rausen, D., Stefanopoulou, A., Kang, J.-M., Eng, J., and Kuo, T.-W., 2005. "A mean value model for control of HCCI engines". *J. of Dyn. Sys., Meas., and Cont.,* **127**(3),
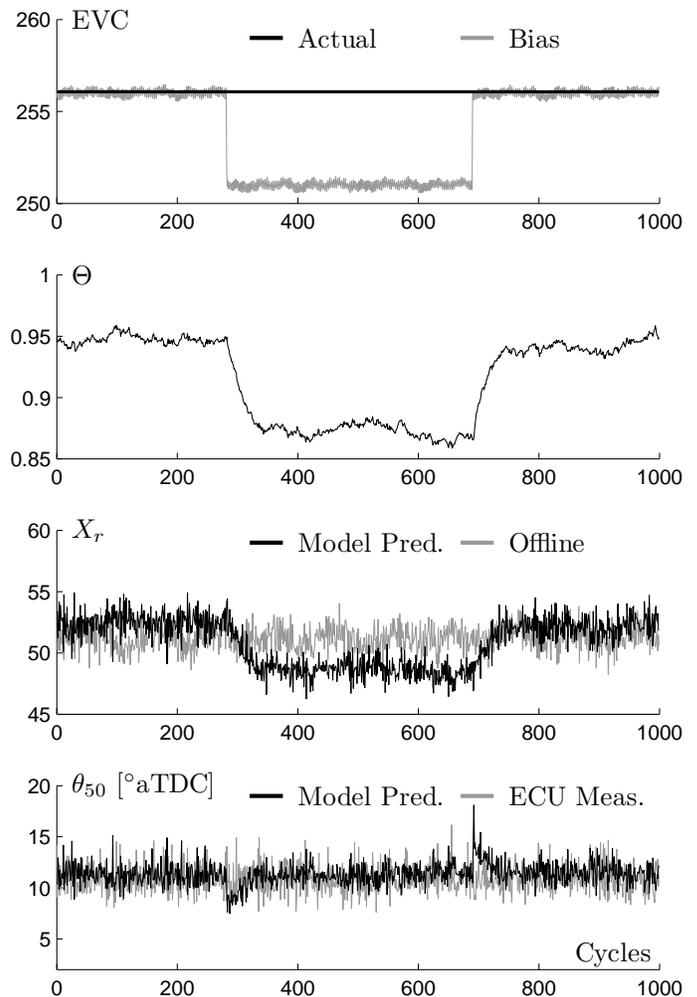
Figure 7. Adaptive model response to an injection of bias in EVC. The model quickly catches the bias and make corrections to minimize error in combustion phasing prediction.

pp. 355–362.

[5] Blom, D., Karlsson, M., Ekholm, K., Tunestål, P., and Johansson, R., 2008. "HCCI engine modeling and control using conservation principles". *SAE paper*(2008-01-0789).

[6] Shahbakhti, M., and Koch, C. R., 2010. "Physics Based Control Oriented Model for HCCI Combustion Timing". *J. Dyn. Syst. Meas. Control,* **132**(2), p. 021010.

[7] Ravi, N., Liao, H., Jungkunz, A., Chang, C., Song, H., and Gerdes, J., 2012. "Modeling and Control of an Exhaust Recompression HCCI Engine Using Split Injection". *J. Dyn. Syst. Meas. Cont.,* **134**, pp. 011016–1–12.

[8] Jade, S., Hellström, E., Stefanopoulou, A., and Jiang, L., 2011. "On the influence of composition on the thermally-dominant recompression HCCI combustion dynamics". In ASME Dynamic Systems and Control Conference.

[9] Jade, S., Hellström, E., Larimore, J., Jiang, L., and Stefanopoulou, A., 2013. "Enabling Large Load Transitions

Copyright © 2013 by ASME

on Multicylinder Recompression HCCI Engines using Fuel Governors". *American Control Conf.* (Accepted).

[10] Bengtsson, J., Strandh, P., Tunestål, P., and Johansson, B., 2006. "Model predictive control of HCCI engine dynamics". *IEEE Int. Conf. Cont. App.*, pp. 1675–1680.

[11] Chiang, C., and Chen, C., 2010. "Constrained control of HCCI engines". *5th IEEE Conf. Indust. Elec. and App.*

[12] Ravi, N., Liao, H., Jungkunz, A., Widd, A., and Gerdes, J., 2012. "Model predictive control of HCCI using variable valve actuation and fuel injection". *Cont. Eng. Prac.,* **20**, pp. 421–430.

[13] Hellström, E., and Stefanopoulou, A., 2011. "Modeling cyclic dispersion in autoignition combustion". In Proc. 50th IEEE Conference on Decision and Control, pp. 6834–6839.

[14] Hellström, E., Larimore, J., Stefanopoulou, A. G., Sterniak, J., and Jiang, L., 2012. "Quantifying cyclic variability in a multicylinder HCCI engine with high residuals". *J. Eng. Gas Turbines and Power,* **134**(11), p. 112803.

[15] Fitzgerald, R., Steeper, R., Snyder, J., Hanson, R., and Hessel, R. "Determination of cycle temperature and residual gas fraction for HCCI negative valve overlap operation". *SAE Int. J. Eng.,* **3**(2010-01-0343), April, pp. 124–141.

[16] Mladek, M., and Onder, C., 2000. "A model for the estimation of inducted air mass and the residual gas fraction using cylinder pressure measurements". *SAE Int.*(23000-01-0958).

[17] Gazis, A., Panousakis, D., Patterson, J., Chen, H., Chen, R., and Turner, J., 2008. "Using in-cylinder gas internal energy balance to calibrate cylinder pressure data and estimate residual gas amount in gasoline HCCI combustion". *Experimental Heat Transfer,* **21**(4), pp. 275–280.

[18] Ortiz-Soto, E., Vavra, J., and Babajimopoulos, A., 2011. "Assessment of residual mass estimation methods for cylinder pressure heat release analysis of HCCI engines with negative valve overlap". Submitted to ASME Internal Combustion Engine Division Fall Technical Conference, 2011.

[19] Larimore, J., Hellström, E., Sterniak, J., Jiang, L., and Stefanopoulou, A., 2012. "Experiments and analysis of high cyclic variability at the operational limits of spark-assisted HCCI combustion". In Proc. ACC, pp. 2072–2077.

[20] Kulenović, M., and Ladas, G., 2002. *Dynamics of Second Order Rational Difference Equations with Open Problems and Conjectures.* Chapman and Hall/CRC.

[21] Grove, E., Ladas, G., McGrath, L., and Teixeira, C., 2001. "Existence and behavior of solutions of a rational system". *Comm. on App. Nonlinear Analysis,* **8**(1), pp. 1–25.

[22] Sedaghat, G., 2000. "Existence of solutions of certain singular difference equations". *Journal of Applied Difference Equations,* **6**(5), pp. 535–561.

[23] Goodwin, G., and Sin, K., 1984. *Adaptive Filtering Prediction and Control.* Prentice-Hall Inf. and Sys. Sci. Ser.

[24] Ioannou, P., and Sun, J., 1996. *Robust Adaptive Control.* Prentice Hall Englewood Cliffs, NJ.

Appendix A: Nomenclature

m_f	Fuel mass per cycle
m_{res}	Trapped residual mass
m_c	Mass of total charge
x_r	Residual gas fraction
η_m	Combustion efficiency
c_v	Specific heat for a given composition
R	Gas constant for a given composition
q_{lhv}	Heating value of the fuel
AFR_s	Stoichiometric air-fuel ratio
SOI	Start of injection
EVO/C	Exhaust valve open/close
IVO/C	Intake valve open/close
NVO	Negative valve overlap
ω	Engine speed
V	Cylinder volume
θ_x	Crank angle of position x
θ_{50}	Measured crank angle of 50% burned
$\hat{\theta}_{50}$	Model prediction of θ_{50}
T	Temperature
P	Pressure
λ	Air-fuel ratio
κ	Forgetting factor
Θ	Adaptive parameter
$T_{ivc,e}$	An estimate of T_{ivc} based on model inversion
cad	Crank angle degrees
RMS	Root mean square

Appendix B: Model Equations

Combustion Phasing Autoignition is predicted using the integrated Arrhenius rate threshold model using a fixed activation temperature $(B = \frac{E_a}{R_u})$ and pre-exponential factor A. The integration is carried out until the threshold (K_{th}) is hit at the start of combustion (θ_{soc}). The model can be expressed as follows:

$$K_{th}(\theta_{soi}) = k_0 - u_{soi} = \int_{\theta_{ivc}}^{\theta_{soc}} \frac{A}{\omega} p_c(\theta)^{n_p} \exp\left(\frac{B}{T_c(\theta)}\right) d\theta \quad (14)$$

The pressure (p_c) and temperature (T_c) of the charge in the cylinder are given by a polytropic compression:

$$p_c(\theta) = p_{ivc}\left(\frac{V_{ivc}}{V(\theta)}\right)^n, \quad T_c(\theta) = T_{ivc}\left(\frac{V_{ivc}}{V(\theta)}\right)^{n-1}. \quad (15)$$

The output θ_{50} is modeled as a linear function of θ_{soc}:

$$\theta_{50} = b_1\theta_{soc} + b_0. \quad (16)$$

For a restricted range of operating conditions, the prediction of combustion phasing can be well approximated by a quadratic whose coefficients vary as linear functions of injection timing:

$$\theta_{50} = \alpha_{\theta1}(soi)T_{ivc}^2 + \alpha_{\theta2}(soi)T_{ivc} + \alpha_{\theta3}(soi) \quad (17)$$

8   Copyright © 2013 by ASME

In-cylinder Temperature Combustion is thermally modeled as an instantaneous heat release at θ_{50} concatenated with a polytropic compression from θ_{ivc} and a polytropic expansion to θ_{evo}. The charge temperature after combustion (T_{ac}) and the temperature rise due to combustion (ΔT) are given by:

$$T_{ac} = T_{ivc}\left(\frac{V_{ivc}}{V_c}\right)^{n-1} + \Delta T \tag{18}$$

$$\Delta T = \eta_m(k)\frac{q_{lhv}m_f(k)}{c_v(k)m_c(k)}$$
$$= \frac{\eta_m(k)q_{lhv}R}{c_v(k)p_{ivc}V_{ivc}}m_f(k)T_{ivc}(k). \tag{19}$$

Here η_m is the combustion efficiency, and n is the polytropic exponent. The specific heat of combustion c_v varies as a function of composition (b_c) to capture variations in mixture properties.

$$\eta_m(k) = \frac{a_0}{1+\exp\left\{\frac{\theta_{50}(k)-a_1}{a_2}\right\}}\left(1+a_3\omega(k)\right) \tag{20}$$

$$c_v(k) = 1 + a_4 b_c(k) \tag{21}$$

Polytropic expansion after combustion gives the charge temperature at θ_{evo}, (T_{evo}), to be:

$$T_{evo}(k) = T_{ac}\left(\frac{V_c}{V_{evo}}\right)^{n-1}$$
$$= T_{ivc}(k)\left(\frac{V_{ivc}}{V_{evo}}\right)^{n-1}\left[1+\frac{\eta_m q_{lhv}RV_c^{n-1}}{c_v p_{ivc}V_{ivc}^n}m_f(k)\right]. \tag{22}$$

Using the ideal gas law, the pressure at θ_{evo} is:

$$p_{evo}(k) = p_{ivc}(k)\frac{V_{ivc}}{V_{evo}}\frac{T_{evo}(k)}{T_{ivc}(k)}$$
$$= p_{ivc}(k)\left(\frac{V_{ivc}}{V_{evo}}\right)^n\left[1+\frac{\eta_m q_{lhv}RV_c^{n-1}}{c_v p_{ivc}V_{ivc}^n}m_f(k)\right]. \tag{23}$$

Expansion is followed by the blowdown process, which is modeled as a polytropic expansion from the pressure at θ_{evo}, (p_{evo}), to the exhaust manifold pressure (p_{em}), with the polytropic exponent n. The temperature at blowdown (T_{bd}) is:

$$T_{bd}(k+1) = T_{evo}(k)\left(\frac{p_{evo}}{p_{em}}\right)^{\frac{1-n}{n}}$$
$$= T_{ivc}(k)\left(\frac{p_{ivc}(k)}{p_{em}}\right)^{\frac{1-n}{n}}\left[1+\frac{\eta_m q_{lhv}RV_c^{n-1}}{c_v p_{ivc}V_{ivc}^n}m_f(k)\right]^{\frac{1}{n}}. \tag{24}$$

Coupling between Cycles

In recompression HCCI a large fraction of the in-cylinder charge is trapped before it can be exhausted. The hot residual gases retained between engine cycles have a significant impact on the temperature and composition of the in-cylinder charge of the subsequent cycle. This internal coupling between cycles is quantified by the residual gas fraction (x_r). In the model presented in [8, 9] the residual gas fraction was a static function for a given

exhaust valve closing timing θ_{evc}, temperature of blowdown gases T_{bd}, engine speed ω, and pressure ratio across the engine Π:

$$x_r(k) = 1 - (c_0 + c_1\theta_{evc})\Pi^{c_2}T_{bd}(k)^{c_3}\omega(k)^{c_4} \tag{25}$$
$$\text{where } \Pi = \frac{p_{im}(k)}{p_{em}(k)}.$$

Thermal Coupling The cooling of the charge from θ_{evo} to θ_{evc} is modeled by a scaling constant c_e. This cooled charge is polytropically compressed and expanded during the NVO region to obtain the residual gas temperature.

$$T_{evc}(k+1) = c_e T_{bd}(k+1) \tag{26}$$

$$T_{soi}(k+1) = T_{evc}(k+1)\left(\frac{V_{evc}}{V_{soi}}\right)^{n-1} - a_4 m_f(k) \tag{27}$$

$$T_{res}(k+1) = T_{soi}(k+1)\left(\frac{V_{soi}}{V_{ivo}}\right)^{n-1} \tag{28}$$

$$T_{res}(k+1) = \left[c_e T_{bd}(k+1)\left(\frac{V_{evc}}{V_{soi}}\right)^{n-1} - a_4 m_f(k)\right]\left(\frac{V_{soi}}{V_{ivo}}\right)^{n-1} \tag{29}$$

The thermal coupling between cycles is modeled by an energy balance equation at θ_{ivc}. The temperature of the hot residuals is assumed to be T_{res} while the rest of the charge is considered to be at the intake manifold temperature (T_{im}). Assuming constant specific heats, an energy balance leads to:

$$T_{ivc}(k+1) = x_r T_{res}(k+1) + (1-x_r)T_{im}. \tag{30}$$

Composition Coupling The burned gas fraction before (b_c) and after (b_{bd}) combustion can be related by simple equations that assume that the fuel combines with a stoichiometric mass of air to form an equal mass of burned gases. Further, an x_r portion of the burned gases is trapped between cycles:

$$b_c(k) = x_r(k)b_{bd}(k) \tag{31}$$

$$b_{bd}(k+1) = \frac{(AFR_s+1)m_f(k)}{m_c(k)} + b_c(k)$$
$$= \frac{(AFR_s+1)R}{p_{ivc}V_{ivc}}T_{ivc}(k)m_f(k) + b_c(k). \tag{32}$$

9